Journal of Mines, Metals and Fuels, *73(8): 2475-2497; 2025. DOI: 10.18311/jmmf/2025/49556*

Print ISSN : 0022-2755

Journal of Mines, Metals and Fuels

Contents available at: *www.informaticsjournals.co.in/index.php/jmmf*

Design and Performance Evaluation of Mechanical Chronometer with Variable Time Delay Arrangement for Safe Evacuation of Mining Workers Using Soft Computing

M. Ardak[1]*, M. Phate[2] and A. Sathe[1]

[1]Mechanical Engineering Department, School of Engineering and Sciences, M. I. T. Art, Design and Technology University, Lonikalbhor, Pune - 412201, Maharashtra, India; mayuri.ardak@gmail.com

[2]Department of Mechanical Engineering, All India Shri Shivaji memorial Society's, College of Engineering, Pune - 412201, Maharashtra, India

Abstract

In environments where electronic systems may fail due to electromagnetic interference or harsh conditions, a mechanically robust chronometer with variable time delay offers a reliable alternative. This study highlights the critical role of mechanical timing devices in enhancing safety for mining evacuation systems, where delayed activation of equipment is essential to protect workers. The design leverages a pallet-escapement wheel mechanism, optimized through CAD modeling and ANSYS simulations, to achieve precise time delays ranging from 20 to 60 minutes. Three pallet weights (450mg, 490mg, and 590mg) and torque values (85,95 and 100N-mm) were tested, with angular twist (20°–280°) as a key input parameter. Experimental results confirm the chronometer's efficacy in ensuring safe evacuation before explosive detonation, validated through mathematical modeling and Response Surface Methodology (RSM). The system's adaptability to variable delays makes it ideal for defense and mining applications where electrical power is unavailable or hazardous.

Major Findings: *Experimental findings shows that the mechanical chronometer is specially designed for the safe evacuation of mining workers before the blast of explosives. The chronometer is designed and its performance models were formulated for getting the best performance. The pin pallet arrangement and escape wheel mechanism is used for getting the variable time delay as per the requirement.*

Keywords: *ANSYS, Mathematical Modeling, Mechanical Chronometer, RSM, Time Delay*

1.0 Introduction

Mechanical chronometers are essential safety devices designed to function independently of electrical power, particularly in critical sectors such as defense and mining. Their ability to operate reliably under extreme conditions such as explosive atmospheres or power failures makes them indispensable for time-sensitive safety applications. In mining environments, they provide a fail-safe delay mechanism to ensure controlled operations, such as detonation, only occur after personnel have been evacuated. Despite advancements in programmable

**Author for correspondence*

digital timers, mechanical time delay mechanisms remain underexplored for safety-critical domains, such as underground mining. This research bridges that gap by introducing a soft computing-optimized mechanical chronometer, contributing a durable, electronics-independent solution applicable to emergency timing control, mine evacuation stages, and fail-safe delay systems in extreme environments.

Aihara *et al.*, [1] Weapons and explosives are powerful and dangerous tools that require strict safety measures to prevent accidental injury or death. Safe and Armed devices are essential safety mechanisms that prevent accidental activation or detonation of weapons and explosives. They come in many different forms, including safety switches, pins, and locking mechanisms, and are used in a variety of applications, from military weapons to law enforcement tools. Proper use and maintenance of safe and armed devices is critical to ensure the safety of personnel and the public. Blumenthal, Aaron S., Michael Nosonovsky[2] Micro-Electro-Mechanical Systems (MEMS) have revolutionized various industries, including defense and military technologies. MEMS sensors, such as accelerometers and gyroscopes, play a crucial role in safety and arming devices, detecting acceleration, angular rate, and orientation changes. Their compact size and integration capabilities make them ideal for military applications, reducing weight and increasing portability. Cvetković *et al*[3]. This study investigates Thomas Earnshaw's escapement mechanism in horology, emphasizing the role of modelling and simulation in understanding historical innovations.Jacob Cowdrey[4], Mechanical clocks have been used for centuries to measure time accurately, relying on various gear systems to transfer energy from a power source to the hands that indicate the time. The design and analysis of gear tooth profiles are crucial for the accuracy, smoothness, and longevity of the clock mechanism. Gopikrishna, and Narsaiah,[5] this literature review examines the design and manufacturing of gear trains, crucial in various industries like automotive, aerospace, robotics, and manufacturing. It discusses methodologies, challenges faced, and potential future. Guo. *et al.*[6], Elastic energy storage is a promising technology that uses materials like springs, rubber bands, or other elastic components to store mechanical energy. Spiral spring devices, also known as torsion springs or clock springs, store potential energy in the form of mechanical stress, which can be released by unwinding or untwisting the spring. Jeong, *et al.*,[7] this literature review focuses on the significance of miniature mechanical safety and arming devices for artillery fuzes in ensuring their safety and effectiveness. The paper discusses the fundamental principles of operation, materials, manufacturing processes, and applications in military and defense contexts. Liang, Zu. and Feng[8]. This literature review emphasizes the importance of dynamic modelling in detecting and diagnosing gearbox faults, crucial for condition monitoring and predictive maintenance of rotating machinery. It covers techniques like vibration analysis, acoustic methods, temperature monitoring, sensor-based techniques, lumped-parameter models, finite element analysis, and system identification techniques. Mei, Tengjiang Hu[9] Micro-Electro-Mechanical Systems (MEMS) have significantly advanced the field of sensors and actuators, particularly in the field of Micro-Electro-Mechanical Systems for Sights and Aiming (MEMS S and A devices). These devices have shown significant progress in miniaturization, precision, low power consumption, and integration with advanced electronics. Milburn[10], this literature review delves into the thermodynamics of clocks, focusing on the relationship between energy, entropy, and precision in timekeeping devices. It examines the historical contribution of early clocks like water and pendulum clocks to modern precision timepieces.Brian M. Naperkoski *et al*[11]. This literature review explores the use of Finite Element Analysis (FEA) in studying the dynamics and performance of mechanical watch lever escapements in traditional mechanical watches. It highlights the importance of FEA in studying mechanical systems and its application in watch making advancements. Gear trains are used in power transmission, torque conversion, and speed control. Phate *et al.*,[12-15] work on response surface methodology in analysis of various engineering process using RSM effectively and effectively. Pook[16], Coiled springs, also known as mainsprings, have been crucial in mechanical systems for centuries due to their ability to store and release energy. They function based on Hooke's law, relating force applied to the spring to resulting deformation. Raza and Wang[17], this literature review examines the use of dynamic simulation in determining the arming distance of the pin pellet runaway escapement, a crucial component of mechanical watches. Rossi, Castellani and

Nicolini[18], mechanical spring systems are a reliable energy storage method known for their high energy density, efficiency, durability, and environmental compatibility. They are suitable for short- to medium-term applications due to their efficiency in energy conversion and minimal losses. Roda-Buch *et.al.,*[19] the Swiss Lever Escapement is a vital part of mechanical watches, controlling the release of energy from the mainspring to the gears. Proper lubrication is crucial for smooth operation, minimizing wear and friction, and maintaining accurate timekeeping. Blumenthal and Nosonovsky[20], the invention of the pendulum revolutionized mechanical clocks by reducing friction and increasing the oscillation period. However, challenges like length adjustment, motion damping, and portability remained. Ugrcic[21], Artillery safety and arming devices are essential for preventing accidental detonation or firing of munitions. They are designed to function flawlessly in extreme conditions, ensuring the safety of military personnel and civilians. WEI Yawei, LI Haojie[22], this literature review explores the design and development of a testing system for evaluating the dynamic arming time of the clock mechanism in fuze safety systems. It emphasizes the importance of precise fuze safety systems in munitions and the need for a reliable testing system.

2.0 Materials and Methods

2.1 Design of Mechanical Chronometer

Mechanical chronometer is a precision timekeeping device designed to for safety device use in mining industries. The position of mechanical chronometer is as shown in Figure 2. Unlike regular watches, which may use quartz crystals or other electronic components for timekeeping, mechanical chronometers rely on intricate mechanical mechanisms.

The various components are

- Escapement mechanism: This mechanism regulates the release of energy from the mainspring to the balance wheel, ensuring a controlled and precise timekeeping motion.
- Mainspring: A coiled spring that stores energy and powers the movement of the watch.
- Gear train: A system of gears that transmits energy from the mainspring to the escapement, controlling the movement of the hands.
- Balance wheel which is a small, weighted wheel that oscillates back and forth, acting as a timekeeping element.

The elements of the mechanical chronometers are as shown in Figure 2 mechanical chronometers can find applications in the mining industry where precise timekeeping is essential for various operational and safety reasons along with synchronization of operations, monitoring shifts and work hours, coordination in exploration and surveying. We selected a mechanical chronometer due to its inherent reliability, immunity to electromagnetic interference, and independence from power sources, which is critical in underground mining environments where electronic systems may fail due to harsh conditions or blast-induced EMI. Moreover, mechanical systems provide a predictable, fail-safe delay

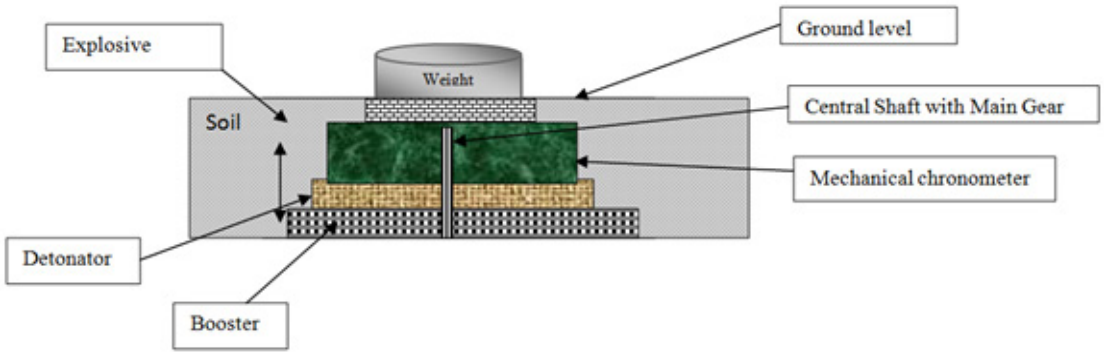


Figure 2. Elements of safety device with mechanical chronometer.

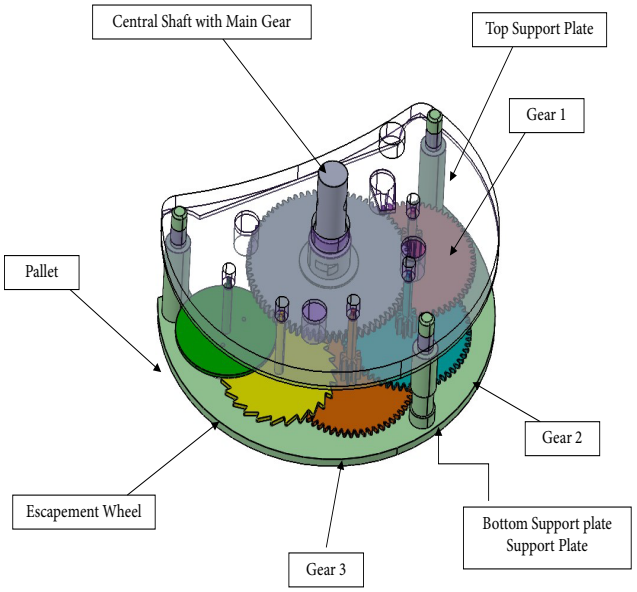


Figure 2. Elements of mechanical chronometer.

mechanism with high durability, and their operability in high-pressure, dusty, and moisture-laden settings makes them a viable choice for time-delay applications in mining safety.

The Mechanical chronometer is "D" shaped , Figure 2 shows the components of the mechanical chronometer assembly, The complete body of the chronometer can be basically divided in 3 parts.viz Top plate contains main central shaft, middle portion containing all moving parts (gears, escapement mechanism, spring) and lastly the base plate contains switches. The novelty of this work lies in the integration of a mechanical pin-pallet escapement-based chronometer with a variable time delay arrangement, tailored specifically for controlled evacuation timelines in mining. Unlike traditional fixed-delay systems, our design allows parametric tuning using physical parameters such as torque and angular twist. Furthermore, the application of soft computing (Response Surface Methodology) for performance evaluation and optimization introduces a systematic, data-driven approach to mechanical chronometer design—an area that has rarely been explored in prior literature.

The central shaft is fitted with a gear which transfers rotational motion initiated by the unwinding of the tensional spring. This torque is transferred from gear to gear through specified gear ratio. This gear ratio is selected for reduction of torque from the first to the last gear. This torque reduction is helpful for regulated energy

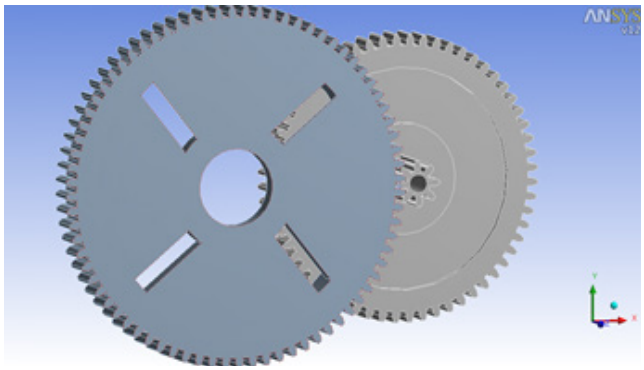


Figure 3. Gear pinion assembly.

dispense by the pallet arrangement. The torque transfer to escape wheel through gear train produces rotational motion about the axis of the escape wheel. This escape wheel is attached to the pallet through two pins of pallet which follows the teeth trajectory of the ratchet. This pallet acts as an energy dispenser which regulates free motion of the ratchet, which in return offers rotational resistance to gears attached to the ratchet and other gear train. This combination in return gives restricted motion to the central shaft or it results in slowly unwinding of the tensional spring irrespective of its wounding speed. The various mechanism uses in the Chronometer is as shown in Figure 2. The gear train is a crucial component of a machine, consisting of a series of gears of different sizes arranged in a sequence. As the first gear rotates due to the unwinding of the clock spring, it transmits torque to the second, third, and so on. Each gear in the sequence has a different gear ratio, allowing it to step down the torque transmitted to the next gear. Static structural analysis has been carried out to check the strength of the first gear pair of the chronometer as spring is attached to the first gear shaft and it exerts maximum load on the pinion when spring is in fully wound condition. These gear pairs reduces torque in further pairing, hence if first pinion is safe then naturally other pinions will also be safe. The pin-pallet escapement was chosen for its simplicity, robustness, and ease of manufacturability. This mechanism enables smooth energy release through controlled oscillation, allowing precise management of time delays without complex feedback circuits. It is highly resistant to jamming or dust interference common in mining applications and facilitates predictable, adjustable delays that can be modulated through pallet geometry and balance wheel dynamics.

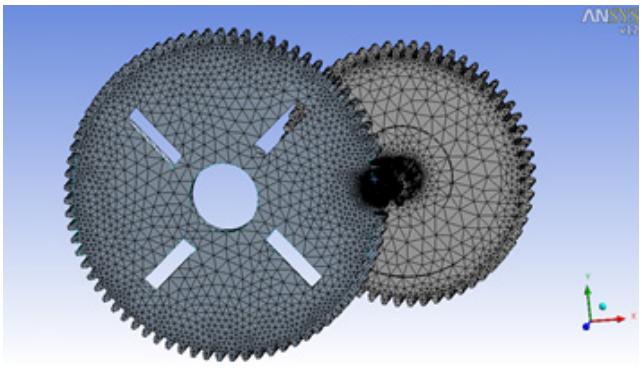


Figure 4. Gear and pinion meshing.

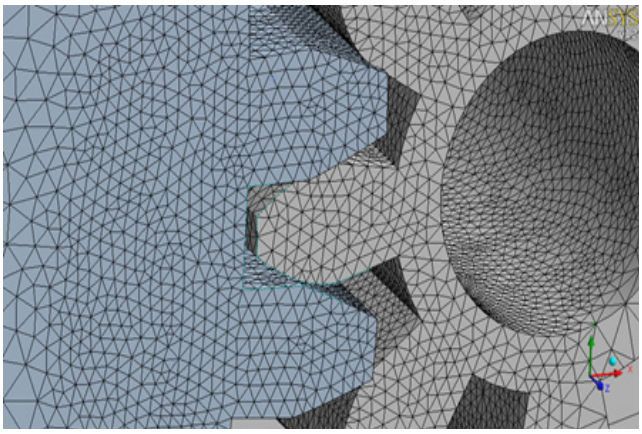


Figure 5. Gear and pinion meshing contact.

The model was developed using solidworks for geometric modelling and ANSYS workbench for simulation and optimization. In the FEA phase, boundary conditions included fixed supports at pivot joints, application of torque on the escape wheel shaft, and contact interaction between pin-pallet and gear teeth. The mechanical properties assigned corresponded to high-carbon spring steel for elasticity and damping accuracy. Uses the default ANSYS workbench shape checking criterion. This criterion has proven to be effective for linear, modal, stress, and thermal problems. A unit less metric is used comparing volume to edge for solid elements and area to edge length for shell elements. Jacobin ratio is also used. If the Jacobin ratio is less than 0 or greater than the limit, then the metric is -1.0 and will cause shape failure. Jacobin ratio is computed at integration points. The parts have been modelled with standard mechanical shape check on.

The parts have been modelled with standard mechanical shape check on. Mesh is refined at and around the contact of the teeth of the gear and pinion. The element size is 0.05 mm at the refined region (Figure 5).

2.2 Loading Conditions

The loading on the central gear by spiral tensional spring is considered with maximum tensional force of 0.05 Nm. The spiral tensional spring exerts near about 0.02 Nm torque, but as our system is dynamic in nature, an additional dynamic factor to this input torque has been considered. The regular dynamic factor consideration is of the order of 1.3. But, a factor of safety is two (2) is being taken into account, hence total dynamic factor will be 2.6. Therefore total input torque is given as,

Total Input Torque = Input Torque X Dynamic Factor
= 0.02 X 2.6
= 0.05 (Nm)

Following Figure 6 shows the loading condition

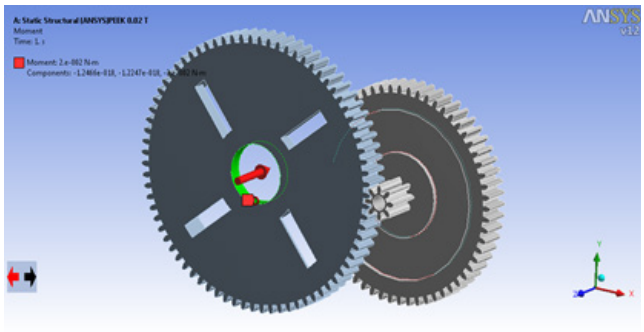


Figure 6. Gear and pinion loading.

2.3 Boundary Conditions

On the first gear shaft hole, frictionless support boundary

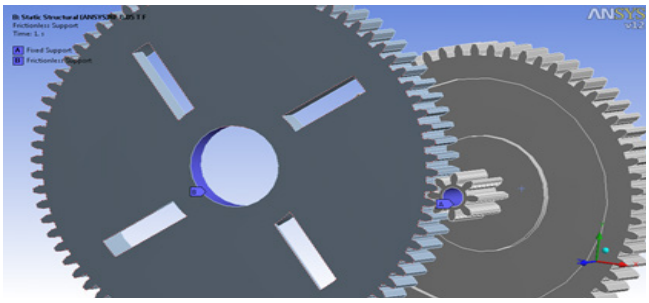


Figure 7. Gear and pinion boundary conditions.

condition is applied, as it is attached to the central shaft. The pinion shaft hole is fixed until the first gear drives it from fixed condition. Boundary conditions are show in following Figure 7.

3.0 Standard Mechanical Shape Check

The ANSYS workbench shape checking criterion is used for linear, modal, stress, and thermal problems. It compares volume to edge for solid elements and area to edge length for shell elements using a unit less metric. The Jacobian ratio is computed at integration points, and if less than 0 or greater than the limit, it causes shape failure.

The housing, located inside the main body cavity, was designed to prevent rotations and translations, ensuring all degrees of freedom were constrained at all nodes on the bottom surface, as illustrated in Figure 8.

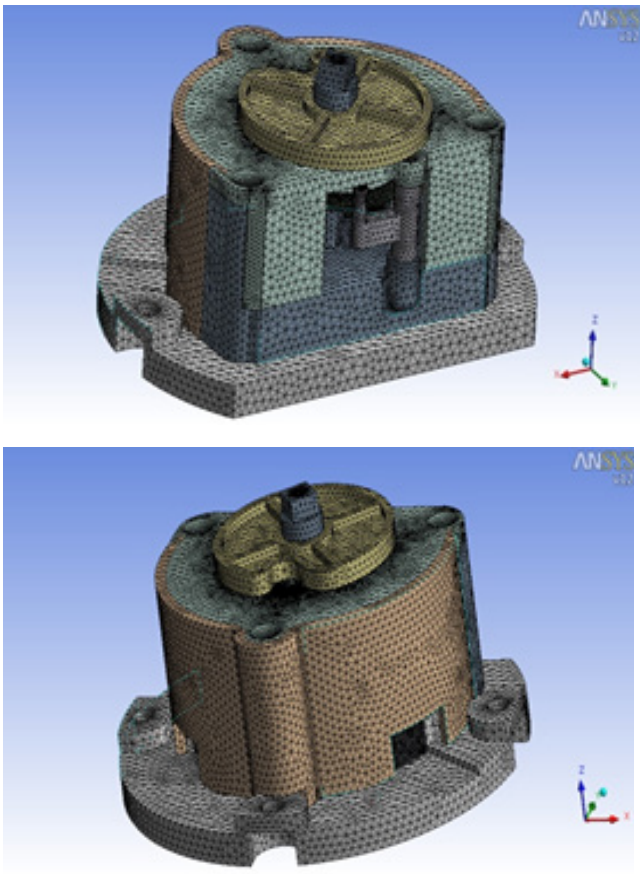


Figure 8. Gear assembly mesh.

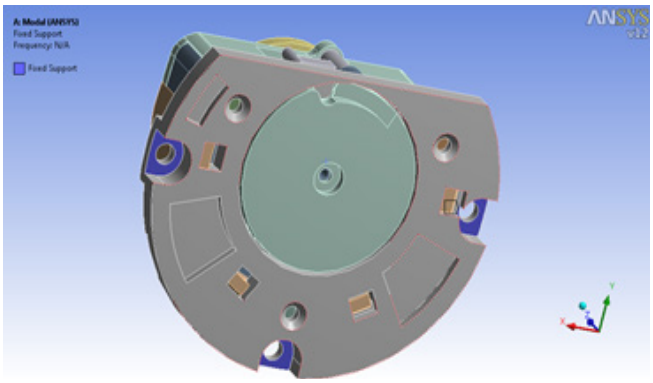


Figure 9. Boundary conditions for stress analysis.

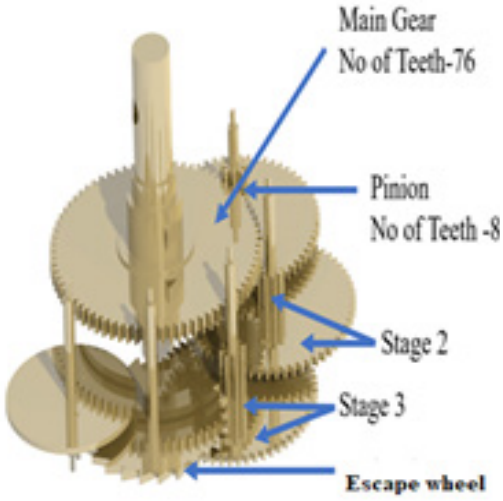


Figure 10. The gear train assembly.

The gear train assembly process involves attaching the main gear to the shaft in the first stage, which meshes with the gears in the second stage. The main gear has 76 teeth, and the second stage has two gears with 60 teeth each. The pinion of the second stage has 8 teeth, and the third stage has another 60-tooth gear. The fourth stage has an 8-tooth gear, and the final element is an escape wheel attached to the same shaft. The assembly process ensures proper alignment and efficiency in the gear train (Figure 10).

We have designed and assembled the gears in the assembly. Escapement mechanism design done and consists of escape wheel with 27 number of teeth and radius of pallet is 6mm. These parameters are such as number of teeth used for escape determines the time delay. This is calculated by considering the motion equations.

After doing the design and assembly of the gear train, further its analysis is carried out to check the failure of the gear train. It is very important to do a study of stress and resulting deformation of the gear train due to them. As any deformation in the gear train will lead to change in time delay provided by the chronometer. So, Static Structural Analysis is done on the gear train or the assembly of the mechanical chronometer. A static structural analysis determines the displacements, stresses, strains, and forces in structures or components caused by loads that do not induce significant inertia and damping effects. Steady loading and response conditions are assumed; that is, the loads and the structure's response are assumed to vary slowly with respect to time. A static structural load can be performed using the ANSYS.

The geometry was imported into the Workbench, but sub-assemblies and components were disturbed, causing interference between gears due to scaling issues. To fix this, the mechanical Chronometer model was repaired in the space claim, preparing it for further analysis (Figure 10).

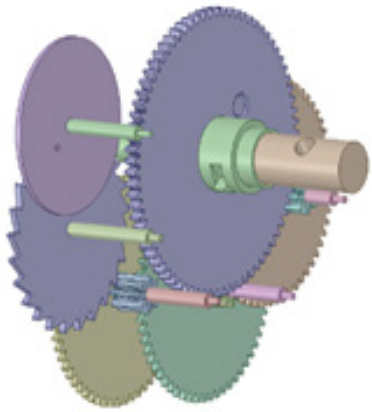


Figure 11. Main gear model.

Table 1. Material specifications

Material Specifications	
Material	**Brass**
Density	$8.73e^{-09}$tonne/mm^3
Young's Modulus	97000 MPa
Thermal Conductivity	0.0605 W/mm°C
Specific Heat	$4.34e^{+05}$ J/tonne°C
Tensile Yield Strength	124MPa

The model is prepared and material properties are added based on industry requirements. The mechanical chronometer is made of brass, which is used for designing the gear train and for static structural analysis. Following (Table 1) are the material modelling properties:

After material modelling next step is to do the meshing of the entire geometry (Table 2). Meshing, also known as mesh generation, is the process of generating a two-dimensional and three-dimensional grid; it is dividing complex geometries into elements that can be used to discretize a domain. We have used tetra mesh for our geometry. A tetrahedral mesh is a 3D generalization of a 2D triangular mesh (Figure 12).

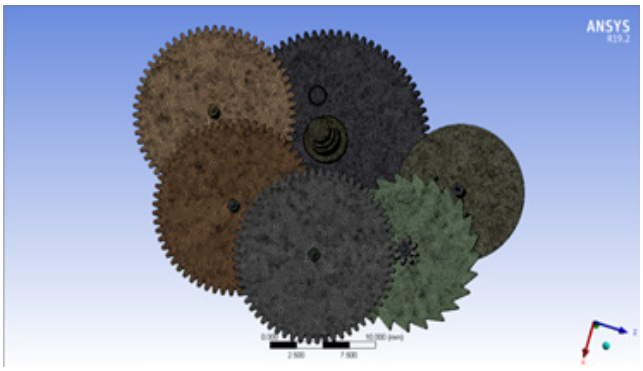


Figure 12. Main gear model.

Table 2. Meshing details

Meshing Details	
Mesh Type	**Tetra**
Mesh Size	0.2mm
Nodes	1389616
Elements	736529

Boundary conditions are constraints assigned to a model, such as applying supports or making any point fixed. They can also include forces, displacement, or moment. Supports represent parts that are not present in the model but interact with it, truncating the domain for numerically accurate results. Different types of support are available, and choosing the appropriate one ensures the simulation model accurately represents the boundary condition. In this case, fixed support is applied to 26 faces

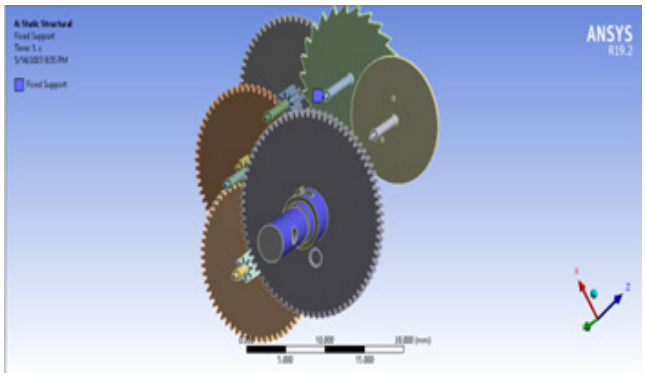


Figure 13. Fixed support.

of the geometry, while moments are applied to the gear face on every stage, with 4 moments applied to the gear face.

It can be observed that sides of the main are constrained as fix and then the faces of shafts of further stages are kept as fix (Figure 13). Loading– Moments are applied on the face of the gears. Every Gear has a different moment applied onto its faces.

Following Table 3 are the details of loading conditions

Table 3. Loading details

Moments on Each Gears	
1st Moment	90 Nmm
2nd Moment	-9.47 Nmm
3rd Moment	1.26 Nmm
4th Moment	-0.0224 Nmm

In the Figure 13, it can be seen that the moment is applied on the main gear. The Moment is applied in the direction based on the direction the escape wheel is desired to rotate. Similarly, as of the main gear the moment is applied on every face of the gear (Figure 14).

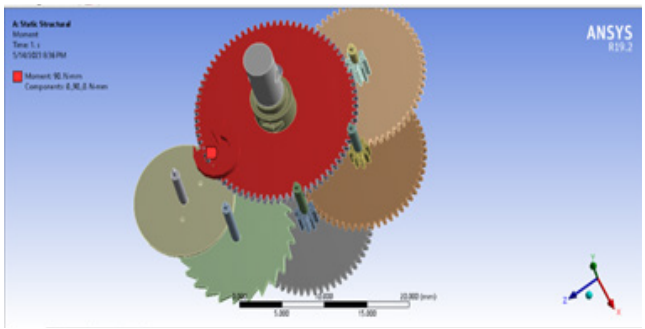


Figure 14. Moments on gear train,

Based on the analysis results it can be seen that the design is safe is safe and there is no failure (Figures 15 and 16). Analysis has pointed some critical region which is at the periphery of the gear 3

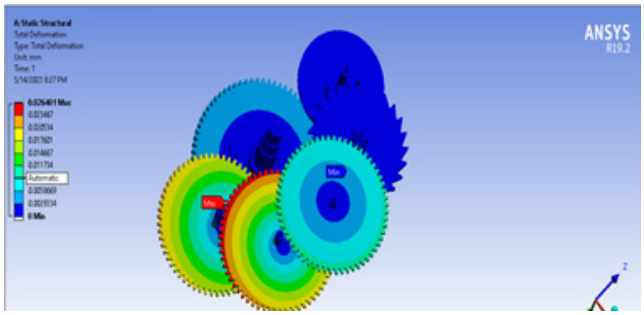


Figure 15. Moments on gear train.

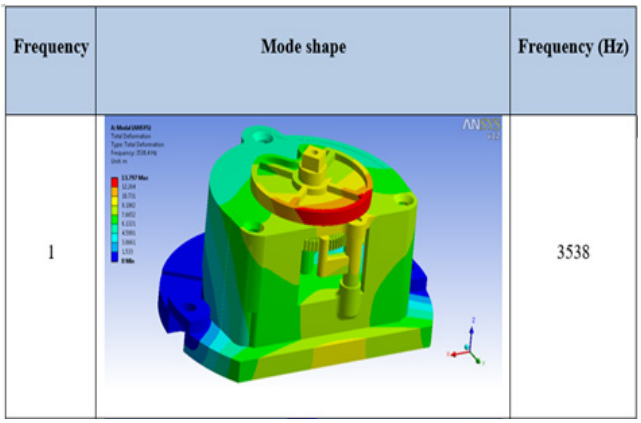


Figure 16. Assembly analysis.

2.2 Experimental Set for Performance Evaluation

The development of a precision test Jig (Figure 17) for mechanical Chronometers is a complex and highly specialized process that involves careful consideration of design, instrumentation, and testing procedures. To design the physical structure of the test jig, including materials, dimensions, and mounting options. Incorporate precision components and mechanisms to simulate the motion and forces experienced by the chronometer during use. Create an environmental chamber that can simulate various conditions like temperature, humidity, and



Mechanical Chronometer | Chronometer Test Bench

Figure 17. Test rig for mechanical chronometer testing.

atmospheric pressure, and integrate a controlled lighting system for marine chronometers.The project involves creating software to manage the test jig, record data, and analyze results, implementing real-time monitoring, and producing detailed test reports with statistical analyses. Develop comprehensive testing procedures that cover all specified parameters and environmental conditions.

2.3 Modelling using Response Surface Method (RSM)

Response Surface Methodology (RSM) is a powerful statistical tool used in engineering, chemistry, and manufacturing to optimize processes and improve product

Table 4. List of final input and output variables

Sr No	Variables	Unit	Notation	Primary Dimensions	Nature	Type	Value
01	Angular Twist	Degree	Θ	$M^0 L^0 T^0 \theta^1$	Input	Varying	Varying
02	Pallet Weight	milligram	PW	$M^1 L^0 T^0 \theta^0$	Input	Varying	Varying
03	Gear Ratio	-----	GR	$M^0 L^0 T^0 \theta^0$	Input	Fixed	7.5
04	Pallet radius	mm	R1	$M^0 L^1 T^0 \theta^0$	Input	Fixed	6
05	Pin radius	mm	R2	$M^0 L^1 T^0 \theta^0$	Input	Fixed	0.2
06	Escape Wheel radius	mm	R3	$M^0 L^1 T^0 \theta^0$	Input	Fixed	7.04
07	Distance between pin 1 & 2	mm	D1	$M^0 L^1 T^0 \theta^0$	Input	Fixed	4.34
08	Distance between pallet to top pin	mm	D2	$M^0 L^1 T^0 \theta^0$	Input	Fixed	2.59
09	Distance between pallet to bottom pin	mm	D3	$M^0 L^1 T^0 \theta^0$	Input	Fixed	2.08
10	Distance between pallet and Escapement wheel	mm	D4	$M^0 L^1 T^0 \theta^0$	Input	Fixed	7.6
11	Tooth angle of last gear (Rachet)	Degree	β	$M^0 L^0 T^0 \theta^1$	Input	Fixed	66.50
12	Escape wheel Tooth half angle	Degree	α	$M^0 L^0 T^0 \theta^1$	Input	Fixed	52.10
13	Spring Torque	N-mm	TQ	$M^1 L^2 T^{-2} \theta^0$	Input	Varying	Varying
14	Gravity constant	m/s^2	g	$M^0 L^0 T^{-2} \theta^0$	Input	Fixed	9.81
14	Time Delay	Sec	TM	$M^0 L^0 T^1 \theta^0$	Output	NA	

performance. By systematically varying input variables (e.g., design and performance parameters) through experimental designs like factorial or box-behnken, RSM builds mathematical models (linear or quadratic) to analyze their effects on response variables. Visualization tools like surface plots help identify relationships, enabling efficient optimization of key outputs. The goal is to determine the best input combinations for desired results, balancing cost and performance. We employed Response Surface Methodology (RSM) to model and optimize the relationship between key design parameters (e.g., torque, angular twist, gear ratio) and performance outputs such as time delay accuracy and oscillation stability. This approach allowed us to develop predictive equations and response surfaces without requiring exhaustive experimentation. It also provided insights into interaction effects and facilitated identification of optimal parameter sets, thereby significantly improving the efficiency and accuracy of the mechanical chronometer design.

The equation used in RSM (Equation 1) typically takes a polynomial form, allowing for the modeling of the relationship between the input variables and the response variable. The general form of the RSM equation for a response 'Y' influenced by 'X' input variables (i.e. X1, X2, X3, ---------, Xk) is as follows:

$$Y = \omega_0 + \sum_{i=1}^{k} \omega_i X_i + \sum_{i=1}^{k} \omega_{ii} {X_i}^2 + \sum_{j=i+1}^{k} \omega_{ij} X_i X_j + \in$$

Equation (1)

Where

- ω_0 =Intercept term
- ω_i = Linear coefficient for the i^{th}input variable
- ω_{ii}= Quadratic coefficient for the i^{th}input variable
- ω_{ij} = Interaction coefficient between the i^{th}input& the j^{th} inputvariable
- X_i& X_j= Level of i^{th} input & the j^{th} input variable
- $\in$ = Error

The coefficients are estimated from the experimental data using techniques such as ordinary least squares regression. The choice of the polynomial degree (linear, quadratic, cubic, etc.) depends on the complexity of the relationships being modeled and is often determined through model selection techniques or prior knowledge about the system. Once the coefficients are estimated, the fitted response surface equation can be used for prediction, optimization, and sensitivity analysis within the range of the experimental design.

3.0 Result and Discussion

Torque and angular twist were selected as primary design variables because they directly influence the energy storage and release mechanism in the spring-barrel assembly of the chronometer. Torque governs the driving force acting on the escapement, while angular twist affects the spring's deformation, influencing timing consistency. By systematically varying these parameters, we could achieve different time delays and optimize the design for precision, thereby enhancing both functional control and mechanical resilience.

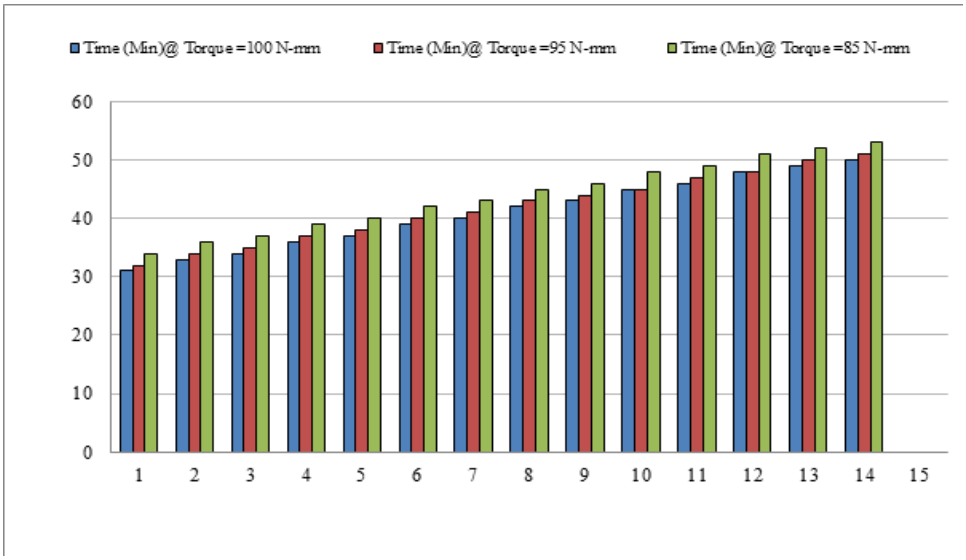
3.1 Modelling and Performance Evaluation of Chronometer with 450mg Pallet

To measure the performance of mechanical Chronometer, three types of Chronometer have been selected based on weight of the pallet. (450mg,490& 590 mg respectively). The performance is measure in terms time delay for the torque of 100N-mm, 95 N-mm and 85 N-mm respectively. The angular twist is taken as an input process parameter (Test points : 20, 40, 60, 80, 100, 120, 140, 160, 180, 200, 220, 240, 260, 280). Different models have been tried using MATLAB. A linear, quadratic and cubic models were tested for the fitting the best one. The models for the 450 mg pallet are tabulated in Table 2. From the results obtain, it is observed that for 450mg pallet weight when the torque is 100 N-mm cubic model with 0.9991 correlation is fitted for the time delay. For the torque is 95 N-mm quadratic model with 0.9989 correlation is fitted for the time delay. For the torque is 85 N-mm cubic model with 0.9991 correlation is fitted for the time delay.

The time delay for the various angular twit test points are tested and compare for the three torque value as mention and the output is compared as shown in Figure 4. From Figure 4, it is observed that the time delay is directly propositional to angular twist and it is maximum at 280 degree angular twist. The model fitted is as given by Equation 2.1 to 3.3.

Table 5. Models for time delay when pallet weight 450 mg

Output	Input	Curve Fitting Type	Correlation
Time Delay (TM)@Torque=100N-mm	Angular Twist (θ)	Linear	0.9987
		Quadratic	0.9990
		Cubic	0.9991
Time Delay (TM)@Torque=95 N-mm	Angular Twist (θ)	Linear	0.9988
		Quadratic	0.9989
		Cubic	0.9954
Time Delay (TM)@Torque=85 N-mm	Angular Twist (θ)	Linear	0.9987
		Quadratic	0.9990
		Cubic	0.9991



Test points	1	2	3	4	5	6	7	8	9	10	11	12	13	14
Angular Twist	20	40	60	80	100	120	140	160	180	200	220	240	260	280

Figure 18. Effect of angular twist on time delay @ 450 gm pallet.

A. Pallet Weight 450 mg

Time Delay (TM)@Torque=100N-mm

Linear Fit : $TM=30+0.074*\theta$, $R2 = 0.9987$ Equation (2.1)

Quadratic Fit : $TM = 29+0.081*\theta-2.2*10^{-5}*\theta^2$, $R2 = 0.9990$ Equation (2.2)

Cubic Fit : $TM = 30+0.07*\theta+6.2*10^{-5}*\theta^2-1.9*10^{-7}*\theta^3$, $R2 = 0.9991$ Equation (2.3)

Time Delay (TM)@Torque=95N-mm

Linear Fit : $TM=31+0.072*\theta$, $R2 = 0.9988$ Equation (3.1)

Pallet weight (milligram)	Run	Angular Twist	Time (Min)@ Torque =100 N-mm	Time (Min)@ Torque =95 N-mm	Time (Min)@ Torque =85 N-mm
450	1	20	31	32	34
	2	40	33	34	36
	3	60	34	35	37
	4	80	36	37	39
	5	100	37	38	40
	6	120	39	40	42
	7	140	40	41	43
	8	160	42	43	45
	9	180	43	44	46
	10	200	45	45	48
	11	220	46	47	49
	12	240	48	48	51
	13	260	49	50	52
	14	280	50	51	53

Quadratic Fit : $TM=31+0.078*\theta-1.7*10^{-5}*\theta^2$, R2 = 0.9989 Equation (3.2)

3.2 Modelling and Performance Evaluation of Chronometer with 490 mg Pallet

The models for the 490 mg pallet are tabulated in Table 3. From the results obtain, it is observed that for 490 mg pallet weight when the torque is 100 N-mm cubic model with 0.9991 correlation is fitted for the time delay. For the torque is 95 N-mm quadratic model with 0.9990 correlation is fitted for the time delay. For the torque is 85 N-mm cubic model with 0.9990 correlation is fitted for the time delay.

Table 7. Models for time delay when pallet weight 490 mg

Output	Input	Curve Fitting Type	Correlation
Time Delay (TM)@Torque=100N-mm	Angular Twist (θ)	Linear	0.9987
		Quadratic	0.9990
		Cubic	0.9991
Time Delay (TM)@Torque=95 N-mm	Angular Twist (θ)	Linear	0.9987
		Quadratic	0.9990
		Cubic	0.9952
Time Delay (TM)@Torque=85 N-mm	Angular Twist (θ)	Linear	0.9987
		Quadratic	0.9978
		Cubic	0.9990

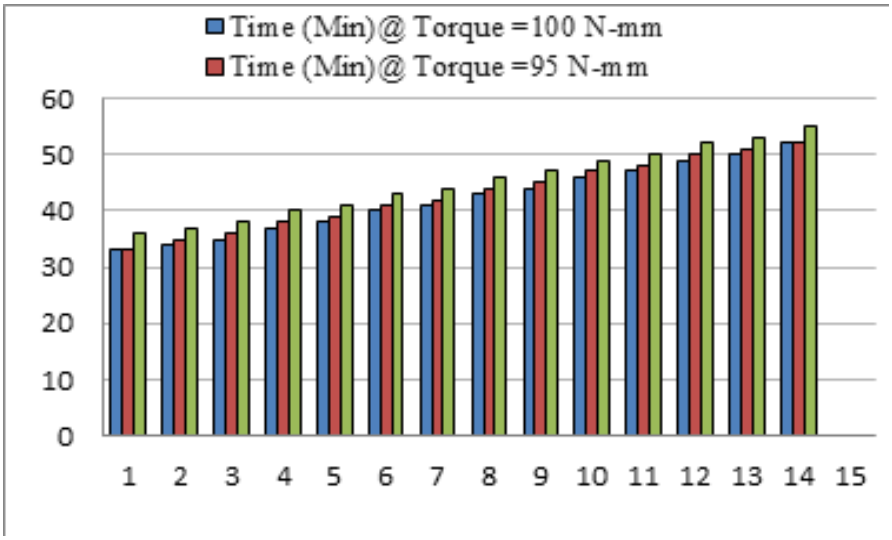


Figure 19. Effect of angular twist on time delay @ 490 gm pallet.

B. Pallet Weight 490 mg

Time Delay (TM)@Torque=100N-mm

Linear Fit : $TM=31+0.074*\theta$,

R2 = 0.9987 Equation (5.1)

Quadratic Fit : $TM=31+0.067*\theta+2.2*10^{-5}*\theta^2$,

R2 = 0.9990 Equation (5.2)

Cubic Fit : $TM=32+0.057*\theta+0.00011*\theta^2-1.9*10^{-7}*\theta^3$,

R2 = 0.9991 Equation (5.3)

Table 8. Impact of angular twist on time delay when pallet weight 490 mg

Pallet weight (miligram)	Angular Twist	Time (Min)@ Torque =100 N-mm	Time (Min)@ Torque =95 N-mm	Time (Min)@ Torque =85 N-mm
490	20	33	33	36
	40	34	35	37
	60	35	36	38
	80	37	38	40
	100	38	39	41
	120	40	41	43
	140	41	42	44
	160	43	44	46
	180	44	45	47
	200	46	47	49
	220	47	48	50
	240	49	50	52
	260	50	51	53
	280	52	52	55

Time Delay (TM)@Torque=95N-mm
Linear Fit : TM=32+0.074*θ,
R2 = 0.9987 Equation (6.1)

Quadratic Fit : TM=31+0.081*θ-2.2*10^{-5} *$θ^2$,
R2 = 0.9990 Equation (6.2)

Cubic Fit : TM=32+0.07*θ-6.2*10^{-5} *$θ^2$-1.9*10^{-7} *$θ^3$,
R2 = 0.9652 Equation (6.3)

Time Delay (TM)@Torque=85N-mm

Linear Fit : TM=34+0.074*θ,
R2 = 0.9987 Equation (7.1)

Quadratic Fit : TM=34+0.067*θ+2.2*10^{-5} *$θ^2$,
R2 = 0.9978 Equation (7.2)

Cubic Fit : TM=35+0.057*θ+0.00011*$θ^2$-1.9*10-7*$θ^3$,
R2 = 0.9990 Equation (7.3)

3.3 Modelling and Performance Evaluation of Chronometer with 590 mg Pallet

C. Pallet Weight 590 mg

Time Delay (TM)@Torque=100N-mm
Linear Fit: TM=34+0.074*θ,
R2 = 0.9987 Equation (8.1)

Quadratic Fit : TM=33+0.081*θ-2.2*10^{-5} *$θ^2$,
R2 = 0.9990 Equation (8.2)

Cubic Fit : TM=34+0.07*θ+6.2*10^{-5} *θ^2-1.9*10^{-7}*$θ^3$,
R2 = 0.9991 Equation (8.3)

Time Delay (TM)@Torque=95N-mm
Linear Fit : TM=35+0.072*θ,
R2 = 0.9988 Equation (9.1)

Quadratic Fit : TM=35+0.078*θ-1.7*10^{-5} *$θ^2$,
R2 = 0.9989 Equation (9.2)

Cubic Fit : TM=34+0.086*θ-8.9*10^{-5} *$θ^2$+1.6*10^{-7} *$θ^3$,
R2 = 0.9990 Equation (9.3)

Time Delay (TM)@Torque=85N-mm
Linear Fit: TM=37+0.074*θ,
R2 = 0.9987 Equation (10.1)

Quadratic Fit : TM=36+0.081*θ-2.2*10^{-5} *$θ^2$,
R2 = 0.9990 Equation (10.2)

Cubic Fit : TM=37+0.07*θ+6.2*10^{-5} *$θ^2$-1.9*10^{-7} *$θ^3$,
R2 = 0.9991 Equation (10.3)

Table 9. Impact of angular twist on time delay when pallet weight 590 mg

Output	Input	Curve Fitting Type	Correlation
Time Delay (TM)@Torque=100N-mm	Angular Twist (θ)	Linear	0.9987
		Quadratic	0.9990
		Cubic	0.9991
Time Delay (TM)@Torque=95 N-mm	Angular Twist (θ)	Linear	0.9988
		Quadratic	0.9989
		Cubic	0.9990
Time Delay (TM)@Torque=85 N-mm	Angular Twist (θ)	Linear	0.9987
		Quadratic	0.9990
		Cubic	0.9991

Table 10. Impact of angular twist on time delay when pallet weight 590 mg

Pallet weight (milligram)	Run	Angular Twist	Time (Min)@ Torque =100 N-mm	Time (Min)@ Torque =95 N-mm	Time (Min)@ Torque =85 N-mm
590	1	20	35	36	38
	2	40	37	38	40
	3	60	38	39	41
	4	80	40	41	43
	5	100	41	42	44
	6	120	43	44	46
	7	140	44	45	47
	8	160	46	47	49
	9	180	47	48	50
	10	200	49	49	52
	11	220	50	51	53
	12	240	52	52	55
	13	260	53	54	56
	14	280	54	55	57

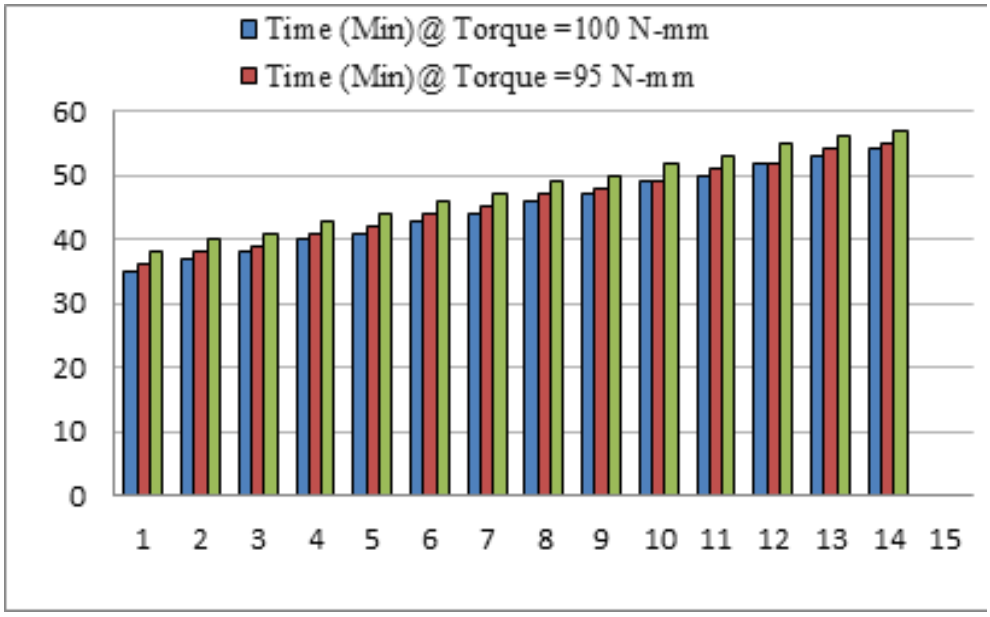


Figure 20. Effect of angular twist on time delay @ 590 gm pallet.

Out of the model formulated quadratic models shows the good performance and commitment. The coefficient represent the influence of main the interaction impact on the time delay. The constant in the model represent the influence of extraneous variables.

3.4 Response Surface Modelling

In this current work, three stages of the research work were essential to analyze the listed performance parameters. In the initial stage of the experimentation various process

Table 11. List of identified process parameters for time delay.

Parameter	Test Envelop													
	1	**2**	**3**	**4**	**5**	**6**	**7**	**8**	**9**	**10**	**11**	**12**	**13**	**14**
AT (Angular twist)	20	40	60	80	100	120	140	160	180	200	220	240	260	280
PW (Pallet weight)	450	490	590	770	820	930	--	--	--	--	--	--	--	--
TQ (Torque)	85	95	100	--	--	--	--	--	--	--	--	--	--	--

Table 12. Impact of various performance parameter on time delay

Run	Coded Input			Uncoded Input			Output
	AT	**PW**	**TQ**	**AT**	**PW**	**TQ**	**TM**
1	1	1	1	20	450	85	34
2	1	2	2	20	490	95	33
3	1	3	3	20	590	100	35
4	2	1	1	60	450	85	37
5	2	2	2	60	490	95	36
6	2	3	3	60	590	100	38
7	3	1	2	120	450	95	40
8	3	2	3	120	490	100	40
9	3	3	1	120	590	85	46
10	4	1	3	180	450	100	43
11	4	2	1	180	490	85	47
12	4	3	2	180	590	95	48
13	5	1	2	240	450	95	48
14	5	2	3	240	490	100	49
15	5	3	1	240	590	85	55
16	6	1	3	280	450	100	50
17	6	2	1	280	490	85	55
18	6	3	2	280	590	95	55

parameters were identified. After fixing the various input process parameters and the target response various experimentation were carried out using Taguchi's L18 mixed plan of experimentation. Finally the experimental was used to carry out the analysis RSM techniques. From the analysis it is observed that the parameters angular twist has major impact followed by the pallet weight and the torque on the response time delay. Figure 21. shows the impact of process parameters on time delay. Time delay is varying directly w.r.t the increase in the angular twist and pallet weight while it goes on decreasing w.r.t to increase in the torque.

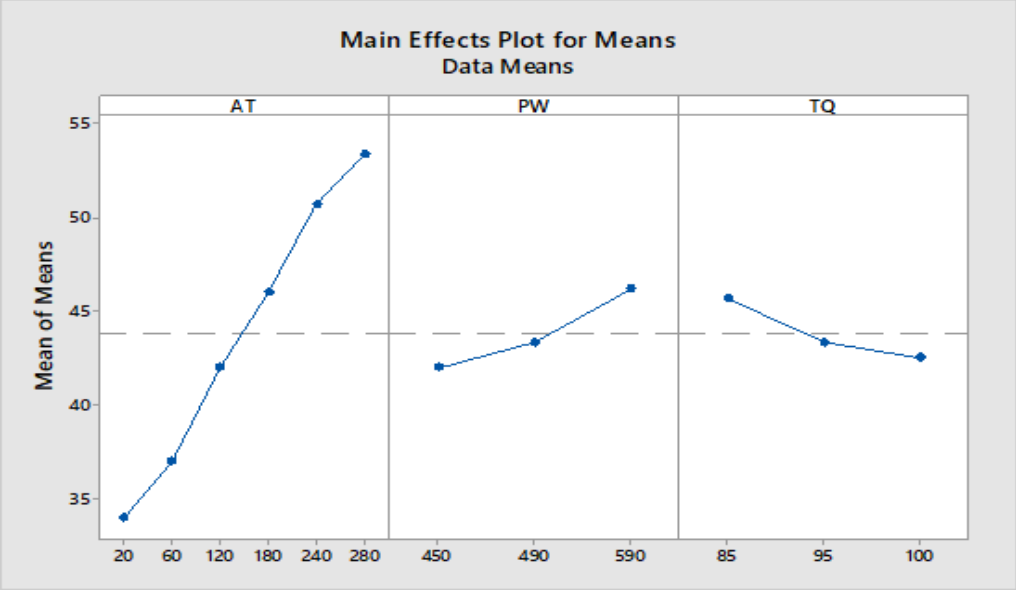


Figure 21. Main effects plots.

Table 13. Analysis of Variance (ANOVA) for time delay

Source	DF	Adj SS	Adj MS	F-Value	P-Value
Model	9	951.663	105.740	1010.18	0.000
Linear	3	773.937	257.979	2464.58	0.000
AT	1	592.866	592.866	5663.90	0.000
PW	1	30.324	30.324	289.69	0.000
TQ	1	17.803	17.803	170.08	0.000
Square	3	0.437	0.146	1.39	0.314
AT*AT	1	0.157	0.157	1.50	0.256
PW*PW	1	0.004	0.004	0.03	0.858
TQ*TQ	1	0.269	0.269	2.57	0.147
2-Way Interaction	3	0.262	0.087	0.83	0.512
AT*PW	1	0.080	0.080	0.77	0.406
AT*TQ	1	0.148	0.148	1.41	0.269
PW*TQ	1	0.112	0.112	1.07	0.331
Error	8	0.837	0.105		
Total	17	952.500			
S	0.323534		R^2 (pred)	0.9954	
R^2	0.9991		R^2 (adj)	0.9981	

The desirability function is used in the optimization section to convert multiple response objectives into a single, comprehensive metric. This approach allows the simultaneous optimization of time delay, energy efficiency, and mechanical stability. It maps each response to a scale from 0 (undesirable) to 1 (most desirable) based on target specifications. This makes it ideal for multi-objective optimization, as it balances conflicting goals, ensuring the chronometer delivers consistent performance under varying operational conditions.

Regression equation in uncoded units

$$TM=71.3+0.0905*AT+0.0600*PW-1.147*TQ-0.000016*AT^2-0.000009*PW^2+0.00601*TQ^2+0.000017*AT*PW-0.000219*AT*PW-0.000267*PW*TQ$$

Equation (11)

Equation 11 defines the empirical relationship between input torque and delay time, fitted using RSM. From this, it is evident that increasing torque reduces delay time nonlinearly, due to higher escapement oscillation frequency. The second-order interaction terms further reveal that minor increases in twist angle can significantly offset torque effects, underscoring the importance of co-optimization.

When interpreting an ANOVA table 9, we focus on the F-ratio and associated p-values to determine whether there are statistically significant differences among the groups being compared. If the p-value is less than the chosen significance level (e.g., 0.05), it is common to reject the null hypothesis and conclude that there are significant differences among the group means. The correlation obtain between experimental and RSM response is 0.9991.

Table 14. Comparative experimental and RSM predicted time delay

Run	Coded Input			Uncoded Input			Output	
	AT	PW	TQ	AT	PW	TQ	TM	TM (RSM)
1	1	1	1	20	450	85	34	33.90
2	1	2	2	20	490	95	33	33.09
3	1	3	3	20	590	100	35	34.96
4	2	1	1	60	450	85	37	37.04
5	2	2	2	60	490	95	36	36.16
6	2	3	3	60	590	100	38	38.06
7	3	1	2	120	450	95	40	39.54
8	3	2	3	120	490	100	40	40.02
9	3	3	1	120	590	85	46	45.88
10	4	1	3	180	450	100	43	43.23
11	4	2	1	180	490	85	47	47.42
12	4	3	2	180	590	95	48	47.90
13	5	1	2	240	450	95	48	48.15
14	5	2	3	240	490	100	49	48.58
15	5	3	1	240	590	85	55	55.04
16	6	1	3	280	450	100	50	50.14
17	6	2	1	280	490	85	55	54.73
18	6	3	2	280	590	95	55	55.16
								0.999560325

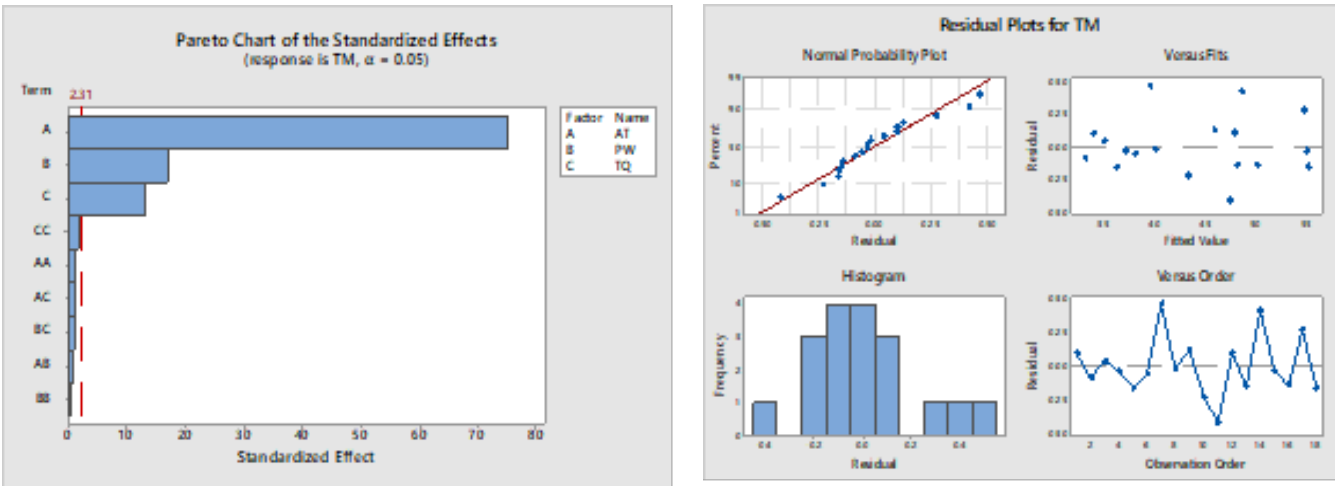
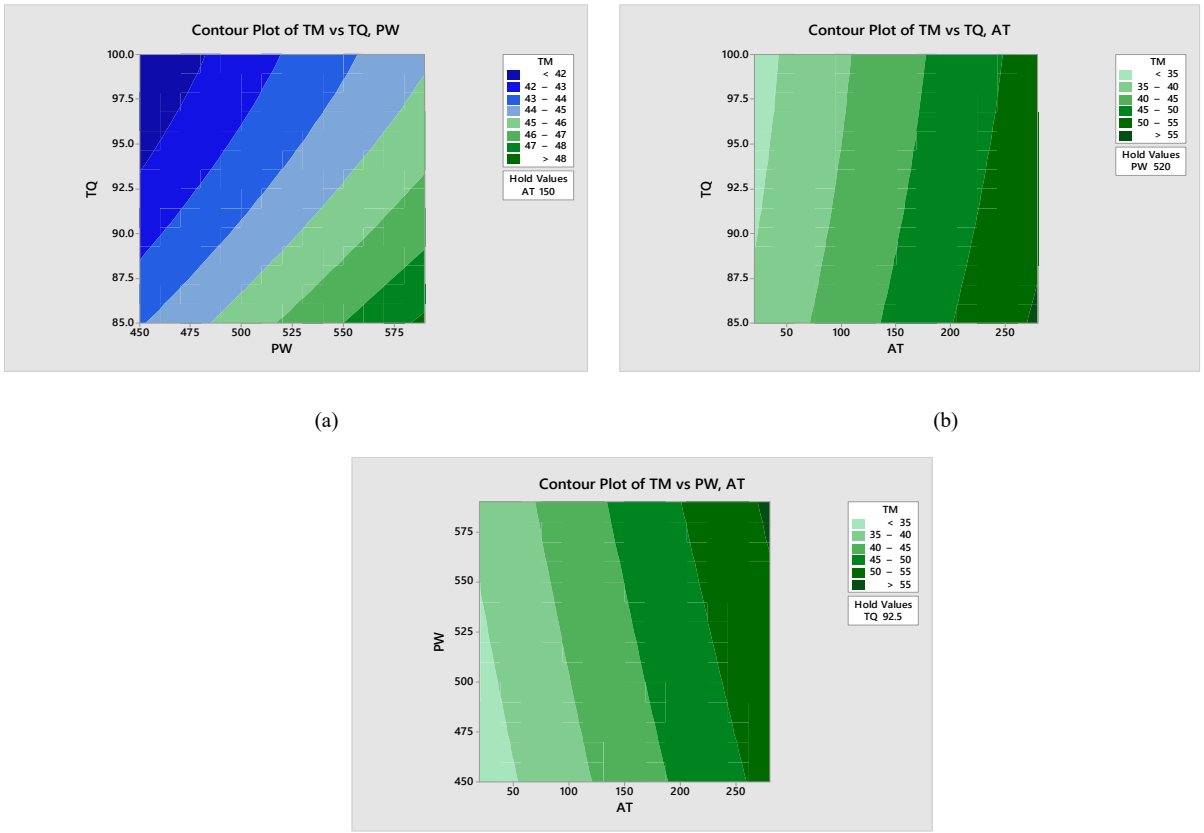


Figure 22. Pareto chart and residual plots for time delay.

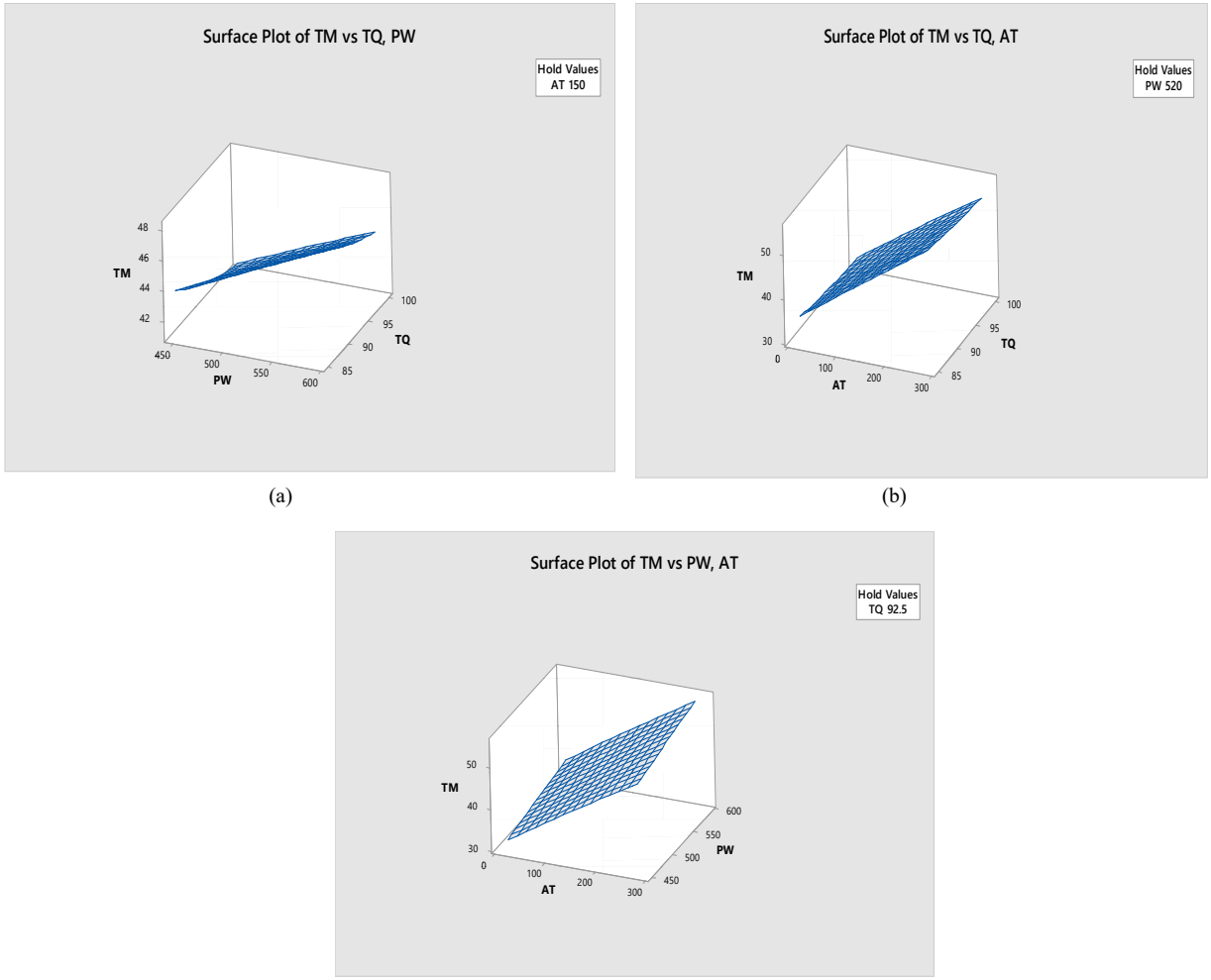


(a) (b)

(c)

Figure 23. Contour plot for time delay.

Pareto chart for the time delay is as shown in Figure 9. It shows the frequencies of various parameters in descending order. The vertical bar represents parameters being analyzed. The height of each bar represents the



(a) (b)

(c)

Figure 24. Response surface plot for time delay.

frequencies of occurrences. Pareto principle is also known as 80/20 rule, means roughly 80% effects come from 20% causes. Hence angle of twist has most significant impact on time delay. Residual plot is also plotted (Figure 22), It shows the goodness of fit for the RSM model. The residuals is the difference between observed and the RSM predicted time delay. It is a scatter plot of residuals.

A contour is plotted for the response time delay. It is a graphical representation of three-dimensional data on a two-dimensional surface. The main feature of a contour plot is the contour lines. These lines connect points on the plot that have the same value. Each contour line represents a constant value of the function being plotted. Between each pair of contour lines, the values of the function change gradually. The spacing between contour lines indicates the rate of change of the function. When contour lines are close together, it indicates a steep gradient or rapid change in the function's value. Conversely, when contour lines are far apart, it indicates a gentle slope or gradual change.The direction of the gradient (the steepest ascent or descent) can be inferred from the orientation of the contour lines. Perpendicular to the contour lines, the gradient is steepest, while parallel to the lines, the gradient is flattest. From Figures 23(a) to 23(c), it is observed that the time delay is gradually change w.r.t. the change in the process parameter PW, TQ and AT.

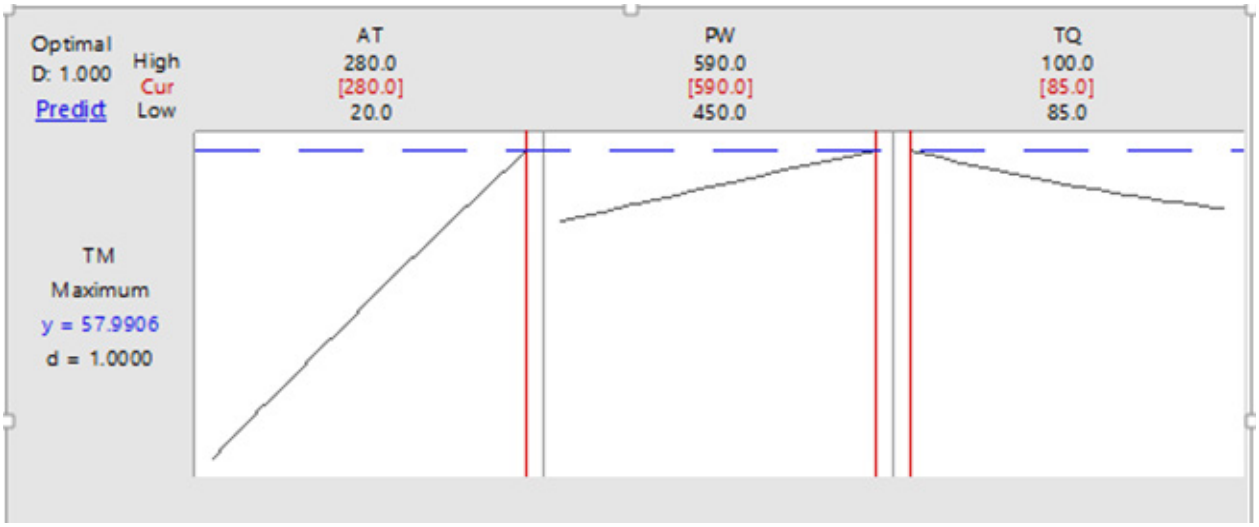


Figure 25. Optimization of time delay.

Surface plots are shown in Figures 24 (a) to 24 (c), it represents the time delay of a RSM model with three process parameters. We can examine how these variables interact with each other to influence the time delay. The peaks and valleys shows the behavior of the time delay w.r.t the process parameters.

3.5 Optimizing the Performance of Mechanical Chronometer

Desirability function is a method of optimization, it combine the multiple objectives into single measure of desirability. In the present work, the objective is to maximize the time delay. For each objective, define a desirability function that maps the objective value to a desirability score between 0 and 1. The desirability function should reflect the importance or preference for different levels of the objective. The desirability plot for maximize the time delay is as shown in following Figure 25.

From the analysis, it is observed that for the best performance of mechanical chronometer the maximum time delay of 57.99 min. The input process parameters are set at Angular twist (280 degree), pallet weight (590 mg) and torque at 85 N-m respectively.

4.0 Conclusion

In the present work, mechanical chronometer is design for the application of in safety and arming device. In mining region there are some particular area or some particular ammunition where certain amount time delay is required. Those ammunition shouldn't function quickly after activation, because that can be harmful for person who is activating particular area. Creation of a mechanical chronometer for generating the necessary time amount of delay and after analyses using the response surface technique have been examined. A chronometer is design and manufacture for time delay. The test rig to test the performance of chronometer is also manufacture and the performance of the chronometer is designed for variable time delay. Various performance models for the time delay along with RSM model is also designed for getting the best performance model. The best performance parameters are also identified for maximizing the time delay. The important parameters like gear ratio, pallet weight, pallet radius, pin radius, escarpment wheel radius, pallet to pin distance, and pallet to escapement wheel distance, and escapement wheel tooth angle were calculated for variable time delay. The optimized performance (maximum time delay) of 57.99 min is obtained when the process parameters are set at angular twist (280 degree), pallet weight (590 mg) and torque at 85 N-m respectively.

The presented work will help to design and set the mechanical chronometer as per the time delay require for the application.

In this Paper we have successfully designed the gear train used in the mechanical chronometer. This gear train

is designed in such a way that it can fit in the casing of the mechanical chronometer. Purpose of the gear train is to transmit the torque or motion from the spring to the last gear which is called as escape. The gear train plays a vital role in achieving the time delay in the mechanical chronometer.

Based on the study of various escapement mechanism we also successfully selected the escapement mechanism to be used in the mechanical. So, the concluded mechanism is Pin pallet escapement mechanism. After the successful selection of the mechanism and designing of the gear train we have performed a Static Structural Analysis on the gear train of the mechanical chronometer.

So, in this way we have successfully designed and developed the gear train used in mechanical chronometer. This research delivers a low-cost, reliable, and power-independent mechanical delay system, critical for staged evacuation during mine emergencies. The integration of mechanical design with soft computing tools ensures that the solution is both highly customizable and environmentally robust. Future applications may extend to fire suppression delays, security time locks, or aerospace deployment systems.

5.0 Acknowledgments

Authors are acknowledged each and every one for direct and indirect support to carry out this work.

6.0 Author contributed to the Manuscript

Conceptualization, MA and MRP methodology, MRP and AS.; software, MA and MRP validation, MRP and AS.; Experimentation, MA resources, MRP and AS.; writing—original draft preparation, MA and MRP.; writing—review and editing, MRP and AS.; supervision, MRP and AS. All authors have read and agreed to the published version of the manuscript**.**

7.0 Declarations

- **Data Availability Statement:** The authors confirm that the data supporting the findings of this study are available within the article [and/or] its supplementary materials.
- **Funding Statement**: No funding was received to assist with the preparation of this manuscript.

8.0 References

1. Aihara T, Kamio C, Hara Y, Ito K, Jujo K. Dynamic accuracy measurement system for mechanical wristwatch. Precis Eng. 2021; 70(9):117-23. https://doi.org/10.1016/j.precisioneng.2021.01.018
2. Blumenthal AS, Nosonovsky M. Friction and dynamics of verge and foliot: How the invention of the pendulum made clocks much more accurate. Appl Mech. 2020; (2):111-22. https://doi.org/10.3390/applmech1020008
3. Cvetković I, Stojicevic M, Popkonstantinović B. Modelling, motion study, and computer simulation of Thomas Earnshaw's chronometer detent escapement mechanism. In: Springer eBooks; 2019. https://doi.org/10.5772/intechopen.73381
4. Cowdrey J. Analysis of gear tooth profiles for use in a mechanical clock [Thesis]. Honors college, Oakland University; 2019.
5. Gopikrishna LR, Narayan S. Design and manufacturing of gear trains. Res J Eng Technol. 2017; 8(4):419-30. https://doi.org/10.5958/2321-581X.2017.00073.3
6. Guo S, Yang L, Yuan Y, Zhang Z, Cao X. Elastic energy storage technology using spiral spring devices and its applications: A review. Energy Built Environ. 2022; 4(6):669-79. https://doi.org/10.1016/j.enbenv.2022.06.005
7. Jeong J, Eom J, Lee SS, Lim DW, Jang YI, Seo KW, *et al.* Miniature mechanical safety and arming device with runaway escapement arming delay mechanism for artillery fuze. Sens Actuators A Phys. 2018; 279:518-24. https://doi.org/10.1016/j.sna.2018.05.040
8. Liang X, Zu MJ, Feng Z. Dynamic modelling of gearbox faults: A review. Mech Syst Signal Process. 2018; 98:852-76. https://doi.org/10.1016/j.ymssp.2017.05.024
9. Li M, Hu T. Research status and development trend of MEMS SandA devices: A review. Def Technol. 2021; 17(2):450-6. https://doi.org/10.1016/j.dt.2020.02.014
10. Milburn GJ. The thermodynamics of clocks. Contemp Phys. 2020; 61(2):69-95. https://doi.org/10.1080/00107514.2020.1837471
11. Naperkoski BM. Exploring the dynamics of a mechanical watch lever escapement using finite element analysis [Thesis]. Virginia polytechnic institute and state university; 2022.
12. Phate MR, Toney SB, Phate VR. Response surface modelling and effective application of adaptive neuro-

fuzzy inference system to analyze surface roughness of Al/Gr/Cp5 MMC. Aust J Mech Eng. 2023; 21(2):653-67. https://doi.org/10.1080/14484846.2021.1913852

13. Phate MR. Comparative analysis of abrasive wear using response surface method and artificial neural network. Inst Eng India Ser D. 2021;102(1):653-67. https://doi.org/10.1007/s40033-021-00250-9
14. Phate MR, Toney SB, Phate VR. Prediction and optimization of tool wear rate during electric discharge machining of Al/Cu/Ni alloy using adaptive neuro-fuzzy inference system. Heliyon. 2020; 6(10):e05161. https://doi.org/10.1016/j.heliyon.2020.e05308 PMid:33163650 PMCid:PMC7610251.
15. Phate MR, Toney SB, Phate VR. Optimization performance parameters of OHNS die steel using dimensional analysis integrated with desirability function. Int J Ind Eng Prod Res. 2020; 30(1):11-23.
16. Pook LP. An introduction to coiled springs (mainsprings) as a power source. Int J Fatigue. 2021; 33(8):1017-24. https://doi.org/10.1016/j.ijfatigue.2010.11.014
17. Raza A, Wang H. Dynamic simulation of pin pellet runaway escapement for determination of arming distance. In: Springer eBooks; 2020. p. 2027-36. https://doi.org/10.1007/978-981-15-8155-7_170
18. Rehan M, Mansoor M. Application of MEMS in safety and arming devices: An overview. Microsyst Technol. 2021; 27(10):3599-610. https://doi.org/10.1007/s00542-020-05162-4
19. Roda-Buch, Magnin V, Maldonado SG, Mischler S. The role of geometrical parameters in the lubrication of the Swiss lever escapement. J Appl Mech. 2021; 88(6):JAM-20-1660. https://doi.org/10.1115/1.4050278
20. Rossi F, Castellani B, Nicolini A. Benefits and challenges of mechanical spring systems for energy storage applications. Energy Procedia. 2015; 82:805-10. https://doi.org/10.1016/j.egypro.2015.11.816
21. Ugrcic M. Clock mechanism as base of artillery safety and arming devices. In: Fracture of Nano and Engineering Materials and Structures, Proceedings of the 16th European Conference of Fracture; 2019.
22. Wei Y, Li H. Design of a testing system for dynamic arming time of clock mechanism in fuze safety system. J Phys Conf Ser. 2020; 1449:012129. https://doi.org/10.1088/1742-6596/1449/1/012129